Environmental Pollution 251 (2019) 502–509

Contents lists available at ScienceDirect

Environmental Pollution

journal homepage: www.elsevier.com/locate/envpol

Benzo[a]pyrene (BaP) exposure generates persistent reactive oxygen species (ROS) to inhibit the NF-κB pathway in medaka (*Oryzias melastigma*)☆

Qian Cui [a], Fang-Yi Chen [a, b, c], Hui-Yun Chen [a, b, c], Hui Peng [a, b, c], Ke-Jian Wang [a, b, c, *]

[a] State Key Laboratory of Marine Environmental Science, College of Ocean & Earth Science, Xiamen University, Xiamen, Fujian, China
[b] State-Province Joint Engineering Laboratory of Marine Bioproducts and Technology, Xiamen University, Xiamen, Fujian, China
[c] Fujian Collaborative Innovation Center for Exploitation and Utilization of Marine Biological Resources, Xiamen University, Xiamen, Fujian, China

ARTICLE INFO

Article history:
Received 19 December 2018
Received in revised form
4 April 2019
Accepted 12 April 2019
Available online 29 April 2019

Keywords:
Benzo[a]pyrene
NF-κB signaling pathway
ROS
ROS-Modulated mechanism

ABSTRACT

Benzo[a]pyrene (BaP), a common environmental pollutant, can modulate the immune-associated signal pathway NF-κB, which is one of the critical signal pathways involved in various immune responses. BaP exposure usually generates reactive oxygen species (ROS), but whether ROS are predominantly involved in the modulation mechanism of the NF-κB pathway has not been clearly understood. In this study, an *in vivo* examination of *Oryzias melastigma* demonstrated that BaP exposure led to a down-regulation of the NF-κB pathway and increased levels of ROS. Conversely, *in vitro* results using the medaka liver cell line DIT-29 and a widely applied H_2O_2 method showed the opposite: up-regulation of the NF-κB pathway. However, the down-regulation of NF-κB upon BaP exposure *in vitro* was inhibited by the addition of a ROS inhibitor, indicating ROS are involved in the modulation of NF-κB. The discrepancy between *in vivo* and *in vitro* results of ROS impacts on NF-κB activation might be related to the concentration and persistence of ROS. Using a modified luminol detection system, BaP was found to generate sustained physiological concentrations of ROS for 24 h, while an H_2O_2 bolus generated ROS for less than 30 min. Furthermore, a steady-state sub-micromolar H_2O_2 system (H_2O_2ss) was developed in parallel as a positive control of ROS, by which H_2O_2 could be maintained for 24 h. Comparative evaluation using H_2O_2, H_2O_2ss and BaP exposures on the medaka cell line with pGL4.32 demonstrated that the persistent physiological concentrations of ROS generated upon BaP exposure or treatment with H_2O_2ss inhibited the NF-κB pathway, but direct H_2O_2 exposure had the opposite effect. Moreover, a western-blot assay and EMSA detection further confirmed the modulation of the NF-κB pathway in DIT-29. Taken together, this study shows that BaP exposure inhibits the NF-κB pathway by generating sustained physiological concentrations of ROS.

1. Introduction

Several studies have indicated that benzo[a]pyrene (BaP) exposure can cause immunotoxicity, for example modulation of the immune system, inhibition of platelet formation, and increased susceptibility to infection by pathogens (Jack, 1994; Smith and Suthers, 1999). In addition to immunotoxicity, BaP exposure is also reported to induce oxidative damage, form DNA adducts, and effect ocular development (Rodd et al., 2017; Huang et al., 2014). Considering BaP is a wildly distributed aromatic hydrocarbon, with reported concentrations in natural seawater ranging from 0.96 to 3.32 μg/L, it's study in marine systems is important for fishery resource management as well as ecological risk assessments (Maskaoui et al., 2002). As reported, BaP usually exerts toxic effects through detoxication and by producing metabolic products through both phase I and phase II metabolism in organisms. A previous study demonstrated that inhibitors of cytochrome P4501A1 (CYP1A1) can reduce BaP-induced immunotoxicity in mammalian cells, inferring that host metabolism may play an important role in regulating BaP's immunotoxic effects (Haggerty and Holsapple, 1990). Cytochrome p450 (CYP) enzymes are important components of phase I metabolism, and ROS are generated during this process (Hernández-García et al., 2010; Regoli and Giuliani, 2014).

☆ This paper has been recommended for acceptance by Christian Sonne.

* Corresponding author. State Key Laboratory of Marine Environmental Science, College of Ocean and Earth Science, Xiamen University, Xiamen, 361005, China.
E-mail address: wkjian@xmu.edu.cn (K.-J. Wang).

https://doi.org/10.1016/j.envpol.2019.04.063
0269-7491/

ROS are known to be side products of oxidative metabolism, and an excessive amount of ROS will lead to the damage of host cells (Xu et al., 2015). ROS can be generated during phagocytosis, indicating the potential effects of ROS in relation to immune responses such as modulating neo-antigens formation and immune associated pathways (Upadhyay et al., 2018). In recent years, many studies have demonstrated that ROS may play a role in modulating a series of signaling pathways, including MAPK, STAT, NF-κB, and others (Nie et al., 2001; Zorov et al., 2014). ROS could be a second messenger of the NF-κB pathway, directing a wide range of immune associated responses, including inflammation, cytokine transcription, bacterial resistance, apoptosis, as well as others (Morgan and Liu, 2011). However, the relationship between ROS and the NF-κB pathway is not necessarily so simple as has been proposed. A review from Nakajima and Kitamura (2013), through comparative analysis of many previously reported ROS-related experiments, indicates that ROS results are dependent on many factors, including the phase chosen to detect, the cytokine used for co-treatment, and even the cell type used (Nakajima and Kitamura, 2013).

It is now known that there are several different forms of ROS which can be converted to one another by way of either an enzymatic reaction or without enzyme participation. H_2O_2, one of the most accessible and storable ROS forms from an experimental perspective, is widely accepted by scientists for studying oxidative stress. In the early stages of ROS studies, researchers typically used a single bolus of H_2O_2 with a concentration of 50–300 μM in their artificial oxidative burst experiments, based on which downstream indicators are detected (Nakajima and Kitamura, 2013). However, the concentration of ROS generated by an organism itself is usually below 10 μM, which is significantly lower than that of ROS detected *in vitro* using H_2O_2 mimicking the "oxidative burst" situation (Sobotta et al., 2013). To our knowledge, the ROS concentration induced by a pollutant exposure including BaP is less than 10 μM due to the limited capability of generating ROS in organisms. Unlike higher concentrations of ROS, which usually induce damage to host cells, low-levels of ROS participate in some critical physiological functions like the modulation of various signaling pathways (Shadel and Horvath, 2015). Previous studies on stem cells have found that a low-level of ROS can activate proliferation pathways, with stem cell proliferation inhibited as ROS levels increase (Schieber and Chandel, 2014).

It is clear that BaP exposure can induce ROS formation, and many studies have shown that BaP exposure can modulate the activity of immune-associated signal pathways such as NF-κB. However, there are often controversial results when observing ROS under different conditions, such as lower or higher concentrations or shorter or longer effective durations. Whether variations in the concentration of ROS will result in different effects on the activity of some signal pathways has not been clearly elucidated yet. While BaP exposure frequently produces lower levels of ROS, researchers prefer to use a relatively higher concentration of H_2O_2 *in vitro* to investigate the effects of ROS, and as a result the conclusions are often unclear. This study aims to elucidate the relationship between the duration of exposure to BaP, ROS concentrations, and regulation of the NF-κB pathway using the marine model fish *Oryzias melastigma*, thus more clearly understanding BaP exposure-induced immunomodulation mechanisms.

2. Materials and methods

2.1. Fish maintenance and exposure

The marine medaka used in this study (a gift from City University of Hong Kong) have been reared for over 10 generations in our laboratory. For each experiment, approximately 120 four-month-old male medaka were randomly transferred to three replicate 20 L tanks for biological replicates. Before exposure to BaP or acetone, medaka were acclimatized in their tanks for 48 h, and the exposures lasted for 5 days. During the experiment, the seawater was kept at a temperature of 26 °C and a salinity of 30‰, and the fish were not fed. Three tanks received 4 nM (1 μg/L) of BaP and three tanks received the same volume of acetone with the exposure media renewed every day for 5 days. The fish were anesthetized by MS-222 (0.25 g/L) before sampling. Acetone and MS-222 has already been demonstrated to have no significant effects (Supporting information). Medaka livers were sampled at time-points of 3 h, 6 h, 12 h, 24 h, 48 h, 72 h, 96 h and 120 h. At least 5 livers were mixed to act as one biological replicate, and then immediately transferred into liquid nitrogen and kept at −80 °C until use.

2.2. Assay of antioxidant enzyme activities and ROS in tissues

The sampled livers were homogenized in a cold saline solution to prepare for assaying the activities of antioxidant enzymes and ROS. The activities of superoxidase dismutase (SOD) and catalase (CAT) in each liver sample were determined using commercial kits (Nanjing Jiancheng Bioengineering Institute, China). SOD activity was assayed using xanthine/xanthine oxidase methods (Superoxide Dismutase (SOD) assay kit) and CAT activity was measured by analyzing the rate of H_2O_2 decomposition at 240 nm (catalase (CAT) assay kit). ROS were measured using dichlorodihydrofluorescein diacetate (DCFH-DA, Sigma-Aldrich). SOD, CAT and ROS were homogenized based on protein concentration, which was detected using a bicinchoninic acid (BCA) assay (ThermoFisher).

2.3. Cell cultures, transfection and luciferase detection

DIT-29, a medaka liver cell line, was purchased from RIKEN BioResource Center and grown in Leibovitz L-15 Media (HyClone) supplemented with 20% fetal bovine serum (FBS) (Gibco) and 10 mM 4-(2-hydroxyethyl)-1-piperazineethanesulfonic acid (HEPES) (Sigma-Aldrich). For luciferase detection, DIT-29 cells were temporally transfected with pGL4.32 (Promega), an NF-κB-RE reporter plasmid, and pRL-TK (Promega), a renilla luciferase control plasmid using Fugen 6 (Promega). The cells were exposed to either BaP, a single bolus of H_2O_2 or steady-state H_2O_2 concentrations (H_2O_2ss), and cultured overnight. Luciferase activity was then measured with a Dual-Luciferase reporter assay System (Promega, Madison, WI).

2.4. Exposure of cells

DIT-29 cells were seeded into 48-well plates to grow for 12 h in a complete medium prior to exposure. All cell line treatments lasted for 24 h.

BaP treatment - BaP was dissolved in dimethyl sulfoxide (DMSO) at a concentration of 1 mM and diluted into cell culture medium at concentrations of 1, 5, 10, 50, 100, and 500 pM. The control groups received the same volume of pure DMSO.

Traditional H_2O_2 treatment (H_2O_2 bolus) - concentrations of H_2O_2 were determined spectrophotometrically ($\varepsilon_{230} = 74\,M^{-1}cm^{-1}$). H_2O_2 was diluted into cell culture medium at concentrations of 20, 50, 100, 200, and 300 μM.

Measurement of H_2O_2 concentrations in cell culture medium-The method used for H_2O_2 determination was modified from Mueller and Arnhold (1995). Briefly, 100 μL of cell culture supernatant from various time-points of the different incubations (BaP, H_2O_2, CAT or GOX) was diluted by a phosphate buffer solution (PBS) (1/100) and added into a white 96-well plate (NUNC). Then, 50 μL of a

0.4 mM luminol in PBS solution was distributed by the first injection channel of the luminometer (Infinite 200 PRO, Tecan), and 50 μL of a 0.12 mM NaOCl solution by the second injection channel. Luminescence was measured immediately after NaOCl injection for over 2 s.

ROS inhibitor treatment - DIT-29 cells were treated with a range of BaP concentrations and either 1 mM N-acetylcysteine (NAC, Sigma) or 0.1 mM 4′-Hydroxy-3′-methoxyacetophenone (Apo, Sigma) at the same time. The control group received the same volumes of DMSO.

Steady State H_2O_2 (H_2O_2ss) treatment - The actual activities of glucose oxidase (GOX, Sigma-Aldrich) were determined by the method described above, using 10 mM glucose at 33 °C. The actual activities of CAT (Sigma-Aldrich) were determined by decomposition of the H_2O_2, which was also quantified at 33 °C. During all experiments, k_{GOX} was kept at 2.8×10^{-8} M/s, whereas k_{CAT} was adjusted to reach defined H_2O_2ss concentrations of 0.5, 1, 2, 3, 4 and 5 μM. The control group also received an extra 10 mM glucose.

DMSO has already been demonstrated to have no significant effects with a range of concentrations (0.00001%–0.00025%) (Supporting information, Fig. S1).

2.5. Measurement and photography of intracellular ROS by DHR123

DIT-29 cells were seeded for 12 h onto an F96 MicroWell™ (NUNC) for the luminometer or a 96 well Glass Bottom Plate with #1 cover glass (Cellvis) for photography and growth. Afterwards, the cells were exposed to BaP, H_2O_2 or H_2O_2ss and loaded with 5 μM Dihydrorhodamine 123 (DHR123, Sigma-Aldrich) 3 h before measurement, and hoechst was loaded onto cells for photography only. 4 × 4 multiple reads were used to eliminate errors caused by cell density for luminometer measurements. Confocal fluorescence imaging was performed with a ZEISS LSM 780 NLO with a 40 × objective lens.

2.6. Preparation of total cell extracts

DIT-29 cells treated under different exposures were lysed in a buffer containing 50 mM Tris-HCl (pH 7.4), 150 mM NaCl, 1% Triton X-100, 1% sodium deoxycholate, 0.1% SDS and 2 μg/mL protease inhibitor. After the cells were vortexed gently for lysis, the cell debris was removed by centrifugation at 2600*g* for 10 min.

2.7. Isolation of nuclear and cytoplasmic extracts

Nuclear and cytoplasmic extractions were prepared using a NE-PER Nuclear and Cytoplasmic Extraction Reagents kit (ThermoFisher) according to the manufacturer's instructions (all incubations were done on ice). Briefly, cells were harvested with trypsin-EDTA, washed twice with cold HBSS and centrifuged at 500 *g* for 3 min 200 μL of Cytoplasmic Extraction Reagent I (CER I) with phenylmethanesulfonyl fluoride (PMSF) was used to suspend cell pellets by vortexing for 15 s. Suspensions were incubated for 10 min followed by the addition of 11 μL of CER II and vortexing for 5 s. After incubating for 1 min, the mixture was centrifuged for 5 min at 16000 *g*. The supernatant fraction (cytoplasmic extract) was transferred to a pre-chilled tube and extracts were stored at −80 °C until use. The insoluble fraction was suspended with ice-cold Nuclear Extraction Reagent (NER) and vortexed for 15 s every 10 min, for a total of 40 min. Then, the suspension was centrifuged for 10 min at 16000 *g*. The nuclear extract was the resulting supernatant, and was stored at −80 °C until use.

2.8. Immunoblotting

The protein concentration of cell extracts was determined by a BCA assay and adjusted to 1 mg/mL in a 4 × SDS buffer with 10% 2-mercaptoethanol. Equal amounts of protein were separated by 10% SDS-polyacrylamide gels and blotted on nitrocellulose membranes. Membranes were blocked in 5% skim milk in Tris-Buffered Saline with Tween (TBST) for 2 h at 37 °C and then incubated in primary antibody (see Table S1) overnight. 5% bovine serum albumin (BSA) in TBST was used for blocking or dilution of the anti-p-RelA antibody. After washing in TBST for 20 min, the secondary antibody was incubated at 37 °C for 1 h followed by another washing step in TBST. The blot was developed using western chemiluminescent HRP substrate (Millipore) and photographed by SYNGENE (Genius).

2.9. Electrophoretic mobility-shift assay (EMSA)

The NF-κB binding site (sequence 5′-AGTTGAGGGGACTTTCC-CAGGC-3′) with a biotin label used as the probe was synthesized and purified by ThermoFisher. The EMSA was performed using a LightShift™ Chemiluminescent EMSA Kit (ThermoFisher) according to the manufacturer's instructions. Briefly, the reaction mixture contained nuclear extracts, binding buffer, glycerol, $MgCl_2$, poly (dI·dC), NP-40 and biotin-NF-κB DNA. After incubation at room temperature for 20 min, the reactions were electrophoresed on 4% polyacrylamide native gels. After transferring binding reactions to a nylon membrane, a UV-light was used to crosslink transferred DNA to the membrane. After washing the membrane with a blocking buffer, washing buffer and Substrate Equilibration buffer in a Chemiluminescent Nucleic Acid Detection Module Kit (ThermoFisher), a Substrate Working Solution was used to incubate the membrane which was then photographed by SYNGENE (Genius).

2.10. Statistical analysis

For the *in vivo* experiment, a student's t-test was used to determine statistically significant differences between each treatment group and its control. One-way ANOVA was used for the *in vitro* experiments to determine statistically significant differences, based on the consideration that there was a range of treatment concentrations applied in those experiments. Data had been tested for normality and homogeneity of variance prior to statistically significant calculation, and the calculation software used was IBM SPSS Statistics 20. Statistically significant differences were accepted at $p < 0.05$.

3. Results

3.1. Effect of BaP on the oxidation-reduction system of medaka

Although BaP is reported to be an oxidative damage inducer, its effects on medaka are still less known. To verify whether BaP exposure could result in oxidative stress to medaka, we used 4 nM of BaP to simulate exposure to water in the natural environment. The activities of the classic antioxidant enzymes CAT and SOD, the amount of ROS, and the regulation of NF-κB and IκB proteins were assessed using medaka liver in the *in vivo* experiments. The activities of CAT and SOD were only significantly up-regulated after exposure to BaP for 3 days in medaka liver (Fig. 1A and B). Concentrations of ROS in the liver (Fig. 1C) were also significantly up-regulated after 3 days. Meanwhile, NF-κB activation in medaka livers during BaP exposure was also assessed (Fig. 1D). Compared with the control group, less Rel A could be phosphorylated, and more of the inhibitor IκBα could be detected by immunoblotting.

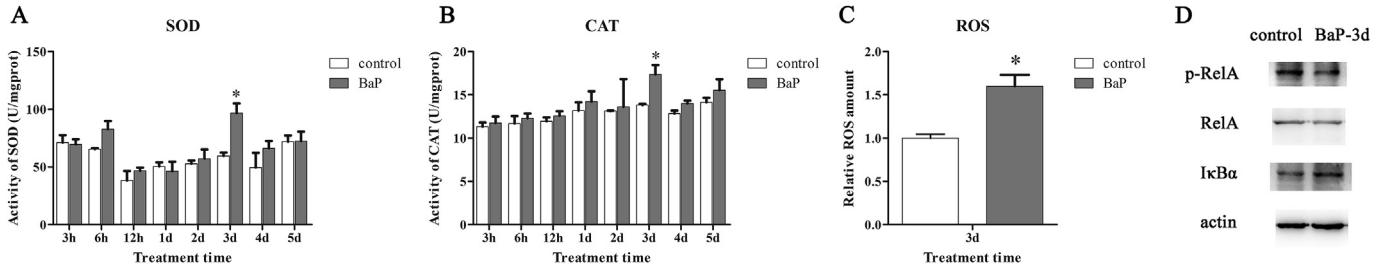

Fig. 1. BaP-induced formation of ROS inhibited the NF-κB pathway in medaka liver. A, B) SOD and CAT enzyme activities were up-regulated after 3 days of BaP exposure. Male medaka were treated with 4 nM BaP and their livers were sampled at different time-points. Each sample for analysis contains at least 5 livers, and 3 samples were analyzed using a SOD or CAT kit. *, $p < 0.05$. C) BaP exposure induced ROS generation in medaka liver after 3 days. 4 samples were analyzed by DCFH-DA. D) Immunoblot analysis of total and phosphorylated RelA, IκBα and IκBβ in lysates of medaka livers with or without BaP treatment.

3.2. BaP had opposite effects compared to H_2O_2 on the NF-κB pathway

To verify the *in vivo* experimental results, which showed that BaP could induce ROS generation and inhibit the NF-κB pathway, we exposed the DIT-29 cell line to BaP. The luminance generated by pGL4.32, whose expression is a function of the activation level of the NF-κB pathway, was significantly suppressed by 1–10 pM of BaP (Fig. 2B). H_2O_2 exposure, which is the classic way to study ROS efficiency, was chosen to be the positive control. However, H_2O_2 activated the NF-κB pathway, especially at concentrations of 50 and 300 μM (Fig. 2A). One explanation for this is that BaP inhibited the NF-κB pathway probably without ROS participation. However, this hypothesis was denied based on results from incubations using the ROS inhibitors Apo and NAC in the study both inhibited the effects of BaP on the NF-κB pathway of the DIT-29 cell line (Fig. S2). Considering the H_2O_2 concentrations used in our experiment, which are considered a conventional choice for *in vitro* experiments but higher than typical physiological levels, we suspect that the ROS concentrations in these two stimulations were different. To

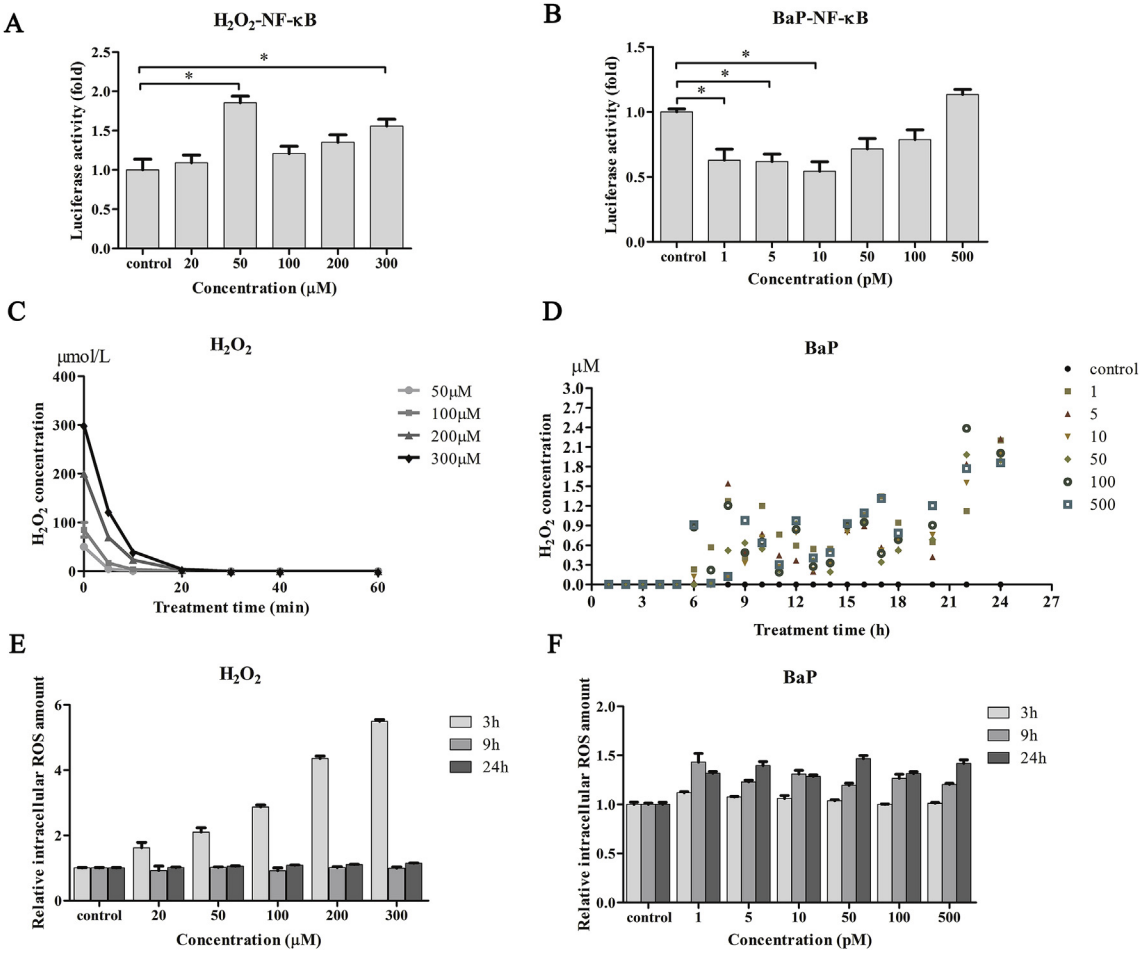

Fig. 2. BaP inhibited the NF-κB pathway through different types of ROS generated by H_2O_2 exposure. A, B) The effects of BaP or H_2O_2 on the NF-κB pathway in DIT-29 cells. Pathway activation was measured by a luciferase assay using a pGL4.32 vector (*, $p < 0.05$). C, D) Extracellular H_2O_2 concentrations over time under BaP or H_2O_2 exposure, detected using a luminol-NaOCl-based chemiluminescence assay. E, F) Intracellular ROS concentrations at different time-points under BaP or H_2O_2 exposure. DIT-29 cells were incubated with DHR123 for 3 h and measured by a microplate reader.

verify this hypothesis, we detected the concentration of ROS in the cell medium. The concentration of H_2O_2 was detectable after BaP exposure for 6 h (Fig. 2D). There was no observable relationship between the BaP exposure concentration and the amount of H_2O_2 generated. However, the H_2O_2 concentration stayed within 0.3–3 μM, inside the range of physiological ROS concentrations. In contrast, the concentration of H_2O_2 rapidly decreased to zero in the cell culture medium by 30 min, consistent with catalase-mediated decomposition by H_2O_2 stimulation (Fig. 2C). Thus, in the direct H_2O_2 exposure experiment, cultured cells were only exposed for a limited time of less than 30 min, in contrast to long-term exposure with BaP.

Considering that direct H_2O_2 exposure could generate oxidative-stress and ROS-induced ROS release (RIRR) in cultured cells, we monitored the intracellular ROS status under BaP vs. H_2O_2 direct exposure. The fluorescence of DHR123 increased within 3 h of H_2O_2 exposure and emerged in a dose-dependent fashion (Fig. 2E). When the exposure time was extended to 24 h, no fluorescence could be observed (Fig. 2E, Fig. S3). Compared with the control group, cells could accumulate about 1.6x intracellular ROS levels in the initial 3 h when exposed to 20 μM H_2O_2, 2x under 50 μM H_2O_2, and 2.8x under 100 μM H_2O_2. BaP exposure could induce ROS generation even after 24 h of exposure, and the microplate reader confirmed there was no dose-dependence between the BaP exposure concentration and the amount of ROS generated (Fig. S4). The microplate reader showed similar results with about 1.4x intracellular ROS observed compared with the control group at all concentrations (Fig. 2F).

3.3. Steady state physiological concentrations of H_2O_2 inhibit the NF-κB pathway

To demonstrate that the different effects of BaP and H_2O_2 on the NF-κB pathway in DIT-29 cells were associated with the amount of and duration of exposure to ROS, we improved on a previously established system to generate steady state H_2O_2 concentrations for at least 24 h *in vitro* (Mueller et al., 2009). The activity of the NF-κB pathway, which was also shown by pGL4.32, was statistically inhibited at 0.5 μM and 1 μM of H_2O_2ss (Fig. 3A). The fluorescence of DHR123 indicated that such low extracellular H_2O_2ss levels can still affect the intracellular ROS status (Fig. 3B). The microplate results showed that steady-state physiological concentrations of H_2O_2 were more efficient at inducing intracellular ROS than direct H_2O_2 exposure over the change of DHR123 fluorescence approaching that induced by 300 μM H_2O_2, even at a concentration of 0.5 μM H_2O_2ss (Fig. 3C). Taken together, the H_2O_2ss system maintained a physiological oxidative-stress environment and suppressed the NF-κB pathway, corresponding to observations during BaP exposure.

3.4. The amount of NF-κB pathway proteins and their phosphorylation were altered under different types of ROS

To support the pGL4.32 results and explore the underlying mechanisms behind these observations, we monitored the total amount and phosphorylation of key NF-κB pathway proteins *in vitro*. Direct H_2O_2 exposure decreased the amount of inhibitor proteins, including IκBα and IκBβ (Fig. 4A), and the phosphorylation of RelA protein increased. In contrast, the amount of IκBα increased at all concentrations under H_2O_2ss exposure (Fig. 4B). The phosphorylation of Rel A was reduced at 0.5 and 1 μM, consistent with the results from pGL4.32. Similar to H_2O_2ss exposure, the phosphorylation of RelA protein was down-regulated by BaP (Fig. 4C), and the amount of IκBα was up-regulated. Additionally, the relative amount of nuclear phosphorylation of RelA, which means more possibilities to modulate downstream genes, was detected and shown to be down-regulated (Fig. 4D). Finally, we detected DNA-binding of the NF-κB pathway by EMSA (Fig. 4E). Binding increased under H_2O_2 exposure but decreased under both H_2O_2ss and BaP exposure.

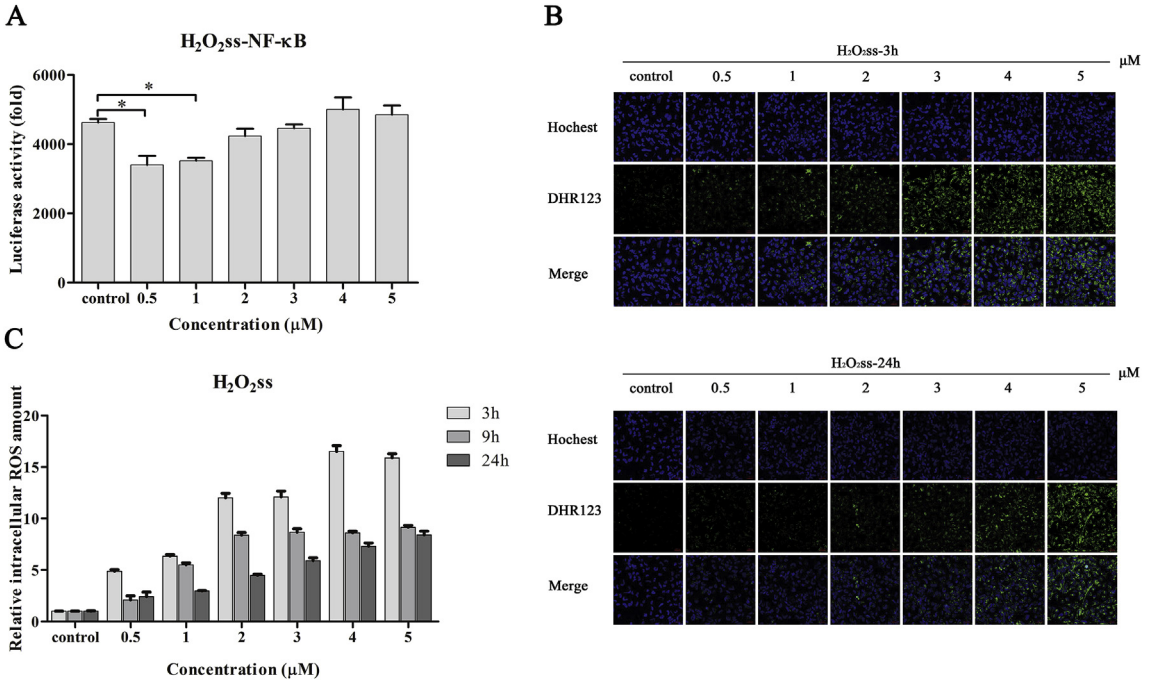

Fig. 3. By generating physiological concentrations of H_2O_2, the steady-state H_2O_2 (H_2O_2ss) treatments inhibited the NF-κB pathway. A) The effects of H_2O_2ss on the NF-κB pathway in DIT-29 cells. Pathway activation was measured by a luciferase assay using a pGL4.32 vector (*, $p < 0.05$). B) H_2O_2ss exposure changed intracellular ROS concentrations within 24 h. Fluorescence was determined by a laser-scanning microscope using the same settings for all conditions. Magnification was 40×. C) Intracellular ROS concentrations at different time-points under H_2O_2ss exposure. DIT-29 cells were incubated with DHR123 for 3 h and measured by a microplate reader.

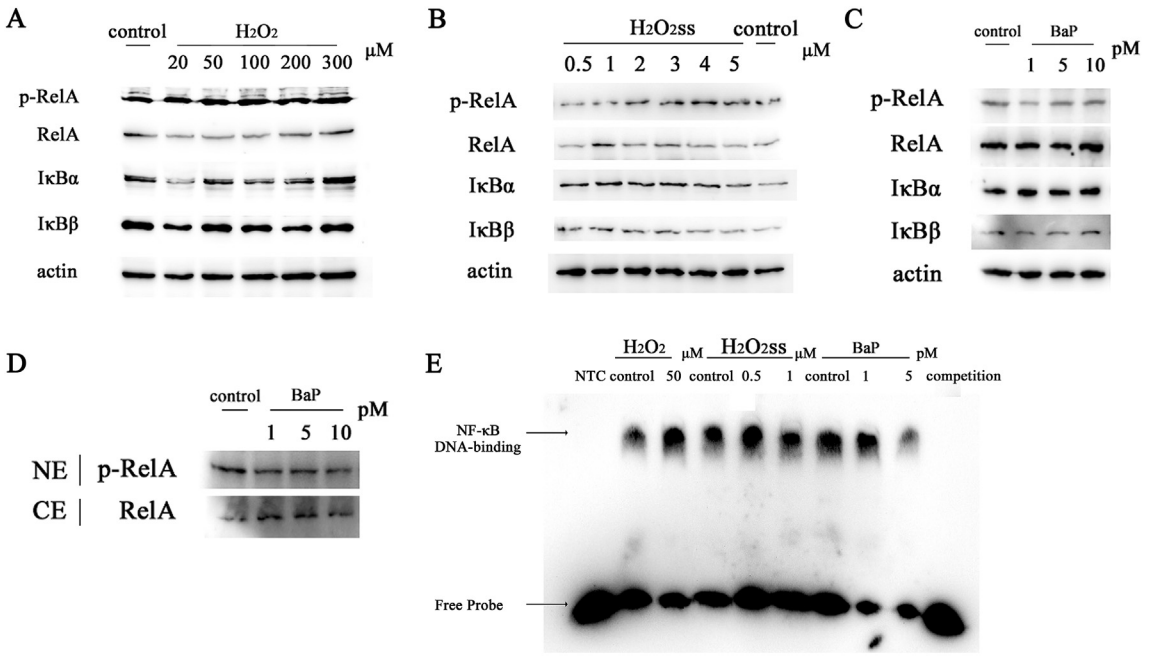

Fig. 4. Concentrations of NF-κB pathway proteins under different exposures. A, B, C) Immunoblot analysis of the indicated proteins in whole-cell lysates of DIT-29 cells stimulated with different concentrations of H_2O_2, H_2O_2ss or BaP. D) Immunoblot analysis of the indicated proteins in the cytoplasmic (CE) and nuclear (NE) extracts of DIT-29 cells under BaP exposure. E) EMSA analysis of the binding of NF-κB to the NF-κB binding site. Nuclear proteins were isolated from DIT-29 cells under H_2O_2, H_2O_2ss or BaP exposure.

4. Discussion

Organisms in the aquatic environment meet various threats, including pollutants, pathogens, and others. Lots of environmental pollutants, including BaP, have been proven to have immunotoxicological effects on mammals and marine animals. Many studies have demonstrated that BaP exposure can result in the generation of ROS, which leads to toxic effects by way of numerous cellular processes. Of these, immunomodulation has been a large concern of researchers, because a change in immune status is closely related to the health of marine animals. However, the multiple variants of ROS, such as O_2^-, RO•, and •OH, as well as their transient nature and ability to interconvert, are barriers for their in-depth study. H_2O_2, a cheap, stable, accessible ROS, has become a widely used reagent for ROS-associated studies (Koman et al., 2016). Many studies have demonstrated that H_2O_2 can activate the NF-κB pathway and involved mechanisms, including formation of the IKK complex, an increase in IKKβ phosphorylation levels, enhancement of DNA-binding, promotion of IκBα degradation, etc. (Nakajima and Kitamura, 2013). It is known that BaP exposure can generate ROS, which are likely involved in the modulation of NF-κB. In our present study, we carried out a ROS inhibitor experiment and found that the regulation of NF-κB is associated with ROS generated during BaP exposure.

However, when we carried out the comparative experiment exposing the DIT-29 cell line to H_2O_2 and BaP, we obtained conflicting results. H_2O_2 can induce the activation of NF-κB as reported previously, but BaP exposure at a range of doses inhibited the activation of NF-κB, demonstrating there is a discrepancy between BaP and H_2O_2 exposure. Therefore, we investigated whether the amount and timeline of ROS generated during these two treatments were likely to be closely associated with the modulation of NF-κB. We developed a modified method to effectively detect lower, instantaneous amounts ROS based on the conventionally used luminol detection system, which has been used in inflammatory studies (Millonig et al., 2012). To our knowledge, this modified luminol detection system was for the first time used to detect the ROS generated by a pollutant, and we found that the amount of ROS generated after BaP was introduced to the DIT-29 cell line was quite lower than after H_2O_2 treatment. The physiological concentrations of ROS produced during BaP exposure ranged from 0.3 to 3 μmol/L, much lower than that produced by H_2O_2 *in vitro*, which was quite higher at 20 μmol/L. Clearly, the conventional method using H_2O_2 *in vitro* in ROS-associated studies would be limited for the toxic effect assessment of BaP exposure, because much lower amounts of ROS are generated by BaP. In fact, there have been several studies indicating that the effect of ROS on NF-κB pathway activity is dependent on the different ROS forms, dosages or exposure periods (Nakajima and Kitamura, 2013). Our conflicting results regarding the effect on NF-κB pathway activity during the H_2O_2 *in vitro* study and BaP exposure *in vivo & in vitro* were probably related to the amount and duration of ROS.

In addition, we carried out a comparative study exposing the DIT-29 cell line to H_2O_2 and BaP, using luminol methods for the detection of extracellular ROS, and DHR123 for the detection of intracellular ROS. The results obtained from both methods showed that the amount and duration of ROS generated upon exposure to BaP or H_2O_2 were inconsistent. Further testing demonstrated that the amount of extracellular ROS generated with H_2O_2 treatment to the DIT-29 cell line diminished to zero within 30 min, whereas the amount of ROS generated upon BaP exposure could maintain a physiological concentration for 24 h. Therefore, our primary results showed that the exposure of the DIT-29 cell line to BaP produced a relatively persistent and lower amount of ROS as compared to the H_2O_2 treatment, which initially produced higher concentrations but only for a short period of time. Through the sustained submicromolar H_2O_2 system (H_2O_2ss) treatment, we can determine that the amount of ROS generated is likely to be a critical factor in the activation of the NF-κB pathway, in addition to those already known.

As an important immune-associated pathway, NF-κB is reported to be associated with cancer, pathogen infection, cell

differentiation, and other biochemical processes. It has been reported that the NF-κB pathway can be regulated by multiple factors, including ROS. Interestingly, in the present study, opposite effects on the NF-κB pathway were observed during H_2O_2 versus BaP exposures. This observation is likely related to the concentration of ROS, which was assessed using a modification of the conventional luminol detection system used for many years by researchers in ROS studies. The modified system was used to observe that H_2O_2 concentrations were only maintained for 30 min in the medium after initially being added. Similarly, Gulden et al. (2010) have shown that H_2O_2 concentrations are only sustained for less than 1 h in a C6 medium, as detected by a xylenol orange assay. Conversely, here we found that ROS could maintain for 24 h after BaP exposure using our modified detection method.

Many previous studies have used H_2O_2 to evaluate the effect of ROS on signaling pathways; however, questions have been raised in recent years on whether *in vitro* experiments using high concentrations of H_2O_2 can be extrapolated to the physiological state (Picard et al., 2011; Yaniv et al., 2013). Although H_2O_2 is usually reported to activate the NF-κB pathway, Khare et al. (2016) have reported that mitochondrial H_2O_2 blocks NF-κB activation. Additionally, concentering complex I was reported to be the main source of ROS in mitochondria based on a catalyzed superoxide production and separation experiment using low NADH concentrations (about 50 μM); however at physiological concentrations of NADH (in the millimolar range) complex I is barely able to carry out this reaction (Grivennikova et al., 2010). These reports corroborate our speculation that the concentration and persistence of ROS generated during BaP exposure should be strongly considered when evaluating ROS effects on the NF-κB pathway, as direct H_2O_2 exposure could not match the toxic effects observed upon BaP exposure. Additionally, we found that Mueller et al. presented a method to investigate the relationship between ROS and the STAT pathway, and that their results are different from those obtained using the conventional H_2O_2 *in vitro* method (Millonig et al., 2012; Mueller and Arnhold, 1995; Sobotta et al., 2013). Because H_2O_2 did not persist for as long as the ROS produced upon BaP exposure, the H_2O_2ss system was developed as a positive control, in which H_2O_2 can maintain a stable and lower level for 24 h, much longer than the 30 min using a bolus of H_2O_2. Using H_2O_2ss as a control, modulation of the NF-κB pathway by ROS generated during the exposure of DIT-29 to BaP could be more reasonably evaluated. In our present study, extracellular ROS concentrations during BaP and H_2O_2ss exposures were kept at a physiological range for 24 h. Although when compared with direct H_2O_2 exposure H_2O_2ss treatments seemed to induce higher intracellular ROS concentrations, this was not the case when the actual accumulation time was taken into consideration. H_2O_2 did not exist for more than 30 min in the medium and was even eliminated within 10 min under 50 μM H_2O_2 exposure. Although we do not know the specific disappearance time for intracellular ROS, we can speculate that the actual accumulation time of intracellular ROS under direct H_2O_2 exposure was also transient, which means the amount of intracellular ROS produced as a function of time was much higher than for H_2O_2ss exposure. In addition, concentrations of intracellular ROS increased along with steady-state H_2O_2 levels while inhibition of the NF-κB pathway disappeared, which provides more proof for the importance of dosage on the efficacy of ROS acting on the NF-κB pathway.

To further investigate whether the modulation of NF-κB pathway activity is dependent on the amount and sustained duration of ROS generated, we first used an NF-κB reporter plasmid (pGL4.32) to compare their effects on the activation of NF-κB during exposure to H_2O_2, H_2O_2ss and BaP. The consistency of the persistence and concentration of ROS between BaP and H_2O_2ss exposures was shown by intracellular and extracellular ROS detection. However, these results also suggest that BaP produces more complicated effects than H_2O_2. Unlike the H_2O_2ss exposures, all ROS detection experiments showed no dose-effect relationships with BaP, and the inhibition effect only appeared at doses of 1–10 pM.

There is a controversy concerning the regulation of the NF-κB pathway by BaP (Tian, 2009). For example, Ajayi et al. (2016) reported that BaP activated the NF-κB pathway of rats based on the up-regulation of RelA protein levels. Lecureur et al. (2005) reported that BaP decreased the DNA-binding amount of the NF-κB pathway in primary human macrophages, but the result was not significant. Hwang et al. (2007) reported that BaP down-regulated the non-canonical NF-κB pathway component RelB in mouse bone marrow-derived dendritic cells. BaP has also been found to inhibit the NF-κB pathway in *Apostichopus japonicas* (selenka) and clams (Li et al., 2016; Su et al., 2017). Additionally, controversial pollutants extend beyond BaP; for example, cadmium has also shown opposite effects on the NF-κB pathway in different studies (Thévenod et al., 2000; Xie and Shaikh, 2006; Yang et al., 2007). The doses, exposure durations, cell lines and/or exposed organisms were different across these studies, and according to these reports and our experimental results, the regulation of NF-κB may be altered by any these factors. This indicates that the regulation of signal pathways by pollutants may require specific, tailored experimental designs.

5. Conclusion

In conclusion, our experiment demonstrated that BaP exposure inhibited the NF-κB pathway in medaka by generating sustained physiological concentrations of ROS. Differences in the modulation of the NF-κB pathway between BaP and direct H_2O_2 exposures are a function of ROS concentrations and the duration of exposure. This article provides a new idea to expound the effect of BaP and ROS on the NF-κB pathway, and a reference for explaining the behavior of similar pollutants.

Associated content

Declarations of interest

None.

Acknowledgement

This work was supported by the National Natural Science Foundation of China [grant numbers 41276102], the Fujian Science and Technology Department [grant numbers 2017NZ0004/2017NZ0004-1], and Fundamental Research Funds from the Central Universities [grant numbers 20720190109]. Dr. Richard W. Smith is thanked for his assistance with English.

Appendix A. Supplementary data

Supplementary data to this article can be found online at https://doi.org/10.1016/j.envpol.2019.04.063.

References

Ajayi, B.O., Adedara, I.A., Farombi, E.O., 2016. Benzo[a]pyrene induces oxidative stress, pro-inflammatory cytokines, expression of nuclear factor-kappa B and deregulation of wnt/beta-catenin signaling in colons of BALB/c mice. Food Chem. Toxicol. 95, 42–51.

Grivennikova, V.G., Kareyeva, A.V., Vinogradov, A.D., 2010. What are the sources of hydrogen peroxide production by heart mitochondria? Biochim. Biophys. Acta 1797, 939–944.

Gulden, M., Jess, A., Kammann, J., Maser, E., Seibert, H., 2010. Cytotoxic potency of H_2O_2 in cell cultures: impact of cell concentration and exposure time. Free Radic. Biol. Med. 49, 1298–1305.

Haggerty, H.G., Holsapple, M.P., 1990. Role of metabolism in dimethylnitrosamine-induced immunosuppression: a review. Toxicology 63, 1–23.
Hernández-García, D., Wood, C.D., Castro-Obregón, S., Covarrubias, L., 2010. Reactive oxygen species: a radical role in development? Free Radic. Biol. Med. 49, 130–143.
Huang, L., Zuo, Z., Zhang, Y., Wu, M., Lin, J.J., Wang, C., 2014. Use of toxicogenomics to predict the potential toxic effect of Benzo[a]pyrene on zebrafish embryos: ocular developmental toxicity. Chemosphere 108, 55–61.
Hwang, J.-A., Lee, J.-A., Cheong, S.-W., Youn, H.-J., Park, J.-H., 2007. Benzo[a]pyrene inhibits growth and functional differentiation of mouse bone marrow-derived dendritic cells: downregulation of RelB and eIF3 p170 by benzo[a]pyrene. Toxicol. Lett. 169, 82–90.
Jack, H.D., 1994. Immunotoxicology and Immunopharmacology. CRC Press.
Khare, A., Raundhal, M., Chakraborty, K., Das, S., Corey, C., Kamga, C.K., Quesnelle, K., St Croix, C., Watkins, S.C., Morse, C., Oriss, T.B., Huff, R., Hannum, R., Ray, P., Shiva, S., Ray, A., 2016. Mitochondrial H_2O_2 in lung antigen-presenting cells blocks NF-kappaB activation to prevent unwarranted immune activation. Cell Rep. 15, 1700–1714.
Koman, V.B., von Moos, N.R., Santschi, C., Slaveykova, V.I., Martin, O.J., 2016. New insights into ROS dynamics: a multi-layered microfluidic chip for ecotoxicological studies on aquatic microorganisms. Nanotoxicology 10, 1041–1050.
Lecureur, V., Ferrec, E.L., N' diaye, M., Vee, M.L., Gardyn, C., Gilot, D., Fardel, O., 2005. ERK-dependent induction of TNFα expression by the environmental contaminant benzo[a]pyrene in primary human macrophages. FEBS Lett. 579, 1904–1910.
Li, C., Zhou, S., Ren, Y., Jiang, S., Xia, B., Dong, X., 2016. Toxic effects in juvenile sea cucumber *Apostichopus japonicas* (Selenka) exposure to benzo[a]pyrene. Fish Shellfish Immunol. 59, 375–381.
Maskaoui, K., Zhou, J., Hong, H., Zhang, Z., 2002. Contamination by polycyclic aromatic hydrocarbons in the jiulong river estuary and western xiamen sea, China. Environ. Pollut. 118, 109–122.
Millonig, G., Ganzleben, I., Peccerella, T., Casanovas, G., Brodziak-Jarosz, L., Breitkopf-Heinlein, K., Dick, T.P., Seitz, H.-K., Muckenthaler, M.U., Mueller, S., 2012. Sustained submicromolar H_2O_2 levels induce hepcidin via signal transducer and activator of transcription 3 (STAT3). J. Biol. Chem. 287, 37472–37482.
Morgan, M.J., Liu, Z.G., 2011. Crosstalk of reactive oxygen species and NF-kappaB signaling. Cell Res. 21, 103–115.
Mueller, S., Arnhold, J., 1995. Fast and sensitive chemiluminescence determination of H_2O_2 concentration in stimulated human neutrophils. J. Biolumin. Chemilumin. 10, 229–237.
Mueller, S., Millonig, G., Waite, G., 2009. The GOX/CAT system: a novel enzymatic method to independently control hydrogen peroxide and hypoxia in cell culture. Adv. Med. Sci. 54, 121.
Nakajima, S., Kitamura, M., 2013. Bidirectional regulation of NF-κB by reactive oxygen species: a role of unfolded protein response. Free Radic. Biol. Med. 65, 162–174.
Nie, M., Blankenship, A.L., Giesy, J.P., 2001. Interactions between aryl hydrocarbon receptor (AhR) and hypoxia signaling pathways. Environ. Toxicol. Pharmacol. 10, 17–27.
Picard, M., Taivassalo, T., Gouspillou, G., Hepple, R.T., 2011. Mitochondria: isolation, structure and function. J. Physiol. 589, 4413–4421.
Regoli, F., Giuliani, M.E., 2014. Oxidative pathways of chemical toxicity and oxidative stress biomarkers in marine organisms. Mar. Environ. Res. 93, 106–117.
Rodd, A.L., Messier, N.J., Vaslet, C.A., Kane, A.B., 2017. A 3D fish liver model for aquatic toxicology: morphological changes and Cyp1a induction in PLHC-1 microtissues after repeated benzo[a]pyrene exposures. Aquat. Toxicol. 186, 134–144.
Schieber, M., Chandel, N.S., 2014. ROS function in redox signaling and oxidative stress. Curr. Biol. : CB 24, R453–R462.
Shadel, G.S., Horvath, T.L., 2015. Mitochondrial ROS signaling in organismal homeostasis. Cell 163, 560–569.
Smith, A., Suthers, I., 1999. Effects of sewage effluent discharge on the abundance, condition and mortality of hulafish, *Trachinops taeniatus* (Plesiopidae). Environ. Pollut. 106, 97–106.
Sobotta, M.C., Barata, A.G., Schmidt, U., Mueller, S., Millonig, G., Dick, T.P., 2013. Exposing cells to H_2O_2: a quantitative comparison between continuous low-dose and one-time high-dose treatments. Free Radic. Biol. Med. 60, 325–335.
Su, W., Zha, S., Wang, Y., Shi, W., Xiao, G., Chai, X., Wu, H., Liu, G., 2017. Benzo[a]pyrene exposure under future ocean acidification scenarios weakens the immune responses of blood clam, Tegillarca granosa. Fish Shellfish Immunol. 63, 465–470.
Thévenod, F., Friedmann, J.M., Katsen, A.D., Hauser, I.A., 2000. Up-regulation of multidrug resistance P-glycoprotein via nuclear factor-κB activation protects kidney proximal tubule cells from cadmium-and reactive oxygen species-induced apoptosis. J. Biol. Chem. 275, 1887–1896.
Tian, Y., 2009. Ah receptor and NF-κB interplay on the stage of epigenome. Biochem. Pharmacol. 77, 670–680.
Upadhyay, S., Vaish, S., Dhiman, M., 2018. Hydrogen peroxide-induced oxidative stress and its impact on innate immune responses in lung carcinoma A549 cells. Mol. Cell. Biochem. 1–13.
Xie, J., Shaikh, Z.A., 2006. Cadmium-induced apoptosis in rat kidney epithelial cells involves decrease in nuclear factor-kappa B activity. Toxicol. Sci. 91, 299–308.
Xu, H.G., Zhai, Y.X., Chen, J., Lu, Y., Wang, J.W., Quan, C.S., Zhao, R.X., Xiao, X., He, Q., Werle, K.D., Kim, H.G., Lopez, R., Cui, R., Liang, J., Li, Y.L., Xu, Z.X., 2015. LKB1 reduces ROS-mediated cell damage via activation of p38. Oncogene 34, 3848–3859.
Yang, P.-M., Chen, H.-C., Tsai, J.-S., Lin, L.-Y., 2007. Cadmium induces Ca^{2+}-dependent necrotic cell death through calpain-triggered mitochondrial depolarization and reactive oxygen species-mediated inhibition of nuclear factor-κB activity. Chem. Res. Toxicol. 20, 406–415.
Yaniv, Y., Juhaszova, M., Sollott, S.J., 2013. Age-related changes of myocardial ATP supply and demand mechanisms. Trends Endocrinol. Metabol. 24, 495–505.
Zorov, D.B., Juhaszova, M., Sollott, S.J., 2014. Mitochondrial reactive oxygen species (ROS) and ROS-induced ROS release. Physiol. Rev. 94, 909–950.